Electron-phonon coupling in metals:
Force constants from tight-binding models

Author
Jesper Möller

Supervisor
Erik van Loon

Co-supervisor
Ali Sufyan

Thesis submitted for the degree of Bachelor of Physics
Project duration: 2 Months

LUND
UNIVERSITY

Department of Physics
Division of Mathematical Physics
May 2026

Acknowledgements

I want to thank both my supervisor Erik and co-supervisor Ali for their time, guidance and support throughout this project. I am grateful for the opportunity to complete my thesis work with them and for all of their valuable insight. I would also like to thank my family and friends for their encouragement and emotional support throughout my studies. Lastly, I acknowledge the use of generative AI to refine parts of the text in this thesis.

Abstract

Electron-lattice interactions play a large role in determining physical properties of crystalline solids, such as electrical resistance and superconductivity. Properties like these are not only of theoretical interest, but also of practical importance when designing new materials. A key quantity describing these interactions is the electron-phonon coupling, which links atomic displacement to changes in the electronic free energy and the resulting lattice forces. This thesis investigates the interatomic force constants emerging from the electron-phonon coupling in a two-dimensional square lattice, within a tight-binding framework. By introducing a distance-dependent hopping parameter, mobile electrons couple to the lattice and the resulting forces can be derived from the electronic structure. The force constants are defined as the second derivative of the Helmholtz free energy of the electronic Hamiltonian. An analysis is given of how variables such as temperature, chemical potential, hopping strength and atomic displacement affects the force constants. Finally, the strength and limitations of this approach to electron-lattice coupling are discussed.

Abbreviations

TB	Tight-binding
TDS	Thermal diffuse scattering
RKKY	Ruderman-Kittel-Kasuya-Yosida
DOS	Density of states

List of Symbols

F	Helmholtz free energy
k_B	Boltzmann constant
T	Temperature
ϵ	Eigenvalue
μ	Chemical potential
Φ	Force constant
S	Entropy
E	Electronic energy
H	Hamiltonian
f_d	Fermi-Dirac function
h	Atomic displacement magnitude
g	A generic function
L_x, L_y	Lattice size in Cartesian directions x and y
c, d	Fitting parameters
α	Parametrization of the coupling strength
t	Hopping amplitude
r	Interatomic distance
N_e	Number of electrons
a	Lattice constant

Contents

1 Introduction

In crystalline solids, the atomic arrangement and their collective motion play a fundamental role in determining material properties. The atoms can be thought of as connected by interatomic springs with a specific force constant. When displaced from their equilibrium position, this consequently causes a cascading movement down the lattice known as phonons, the quantized units of lattice vibrations. The phonon dispersion is determined by these force constants, which encode the stiffness of the lattice. These effective spring constants include both direct interatomic interactions and interactions mediated by electrons, the latter being the central focus of this thesis.

In solids, one of the key distinctions is between metals and insulators. In an insulating material, all electronic states below the band gap are filled, leading to strongly suppressed charge transport. On the other hand, in metals the states are occupied up to a partially filled band, meaning there are always available states arbitrarily close.

In metals, interactions between mobile electrons and lattice vibrations, commonly referred to as electron-phonon coupling, are one of the main reasons behind properties such as electrical resistivity and thermodynamic effects [1]. This implies that the forces acting on atoms include contributions arising from electron-mediated interactions, in addition to the purely mechanical interatomic interactions. For metallic systems, electron-mediated interactions can become long-ranged and oscillatory, as seen in Friedel-type screening [2], which produces oscillatory charge-density responses around perturbations, and Ruderman-Kittel-Kasuya-Yosida (RKKY)-like couplings [3–5], where conduction electrons mediate oscillatory spin-spin exchange interactions between localized magnetic moments. This distinction between metallic versus insulating materials is discussed by Walter Kohn in the Theory of the insulating state [6] from 1964.

Descriptions of electron-lattice systems are often based on the Born-Oppenheimer approximation, formulated by Max Born and J. Robert Oppenheimer in 1927 [7]. This states that due to the large mass difference between electrons and nuclei, their motions can be separated. Within this approximation, the electronic structure is solved for fixed atomic positions and the resulting energy defines a potential energy surface for the atomic motion. This allows phonons to be treated as dynamics of ions moving in an electronic landscape, providing a connection between electronic structure and interatomic forces.

A simple, but powerful, way of modelling electrons is through the tight-binding model, where electrons are assumed to be bound to the atoms, but able to hop between neighboring atomic sites. Despite being a simple model, this captures the essential features of electronic band structure and can provide an efficient way compared to other more demanding first-principles methods [8,9]. By allowing the hopping amplitudes to depend on interatomic distance, we consequently incorporate the effects of electron-phonon coupling.

In this thesis we analyze the resulting force constants and what variables govern both their strength and decay within a tight-binding lattice model simulating a simple metal, using custom-made numerical code. The main idea is to evaluate the Helmholtz free energy of the atomic system as a function of atomic displacements around equilibrium positions, and to obtain the resulting force constants between atomic pairs from the second derivatives

of this energy. The aim is to analyze the force constants dependence on systemic variables such as temperature, chemical potential, hopping strength and displacement magnitude. We also discuss the limitations of the model and to what extent it can capture lattice properties.

A related experimental approach to extracting lattice properties is thermal diffuse scattering (TDS) of X-rays [10], where phonon properties are indirectly obtained from diffuse scattering data. In contrast to Bragg diffraction, which detects long-range periodic order through sharp diffraction peaks, TDS arises from thermal lattice vibrations that provide continuous intensities related to phonon excitations. Modern synchrotron based experiments have demonstrated that TDS can be used to retrieve phonon dispersion relations by fitting measured intensity patterns to lattice models, such as the Born von Karman force constant model [10]. This inverse problem, where measurable quantities are related to force constants through model-dependent properties, shares a conceptual approach with this work.

The structure of this thesis is as follows: Section 2 covers necessary theoretical background, where we introduce the tight-binding approximation for a two-dimensional square lattice and its thermodynamic formulation based on the Helmholtz free energy. Emphasis is put on the role of distance-dependent hopping and how it relates to electron-phonon coupling. Later, in section 3, we present the computational methodology used, including construction and diagonalization of the tight-binding Hamiltonian, evaluation of the finite-temperature free energy, and numerical extraction of interatomic force constants using finite displacements. We also discuss simplifications due to symmetries originating from lattice periodicity and how these can be implemented. In section 4, the main numerical results are presented and discussed, including total energy based on atomic displacement, spatial structure of the real force constant matrix and the temperature and chemical potential dependence of the resulting forces. Finally, section 5 contains a summary of the results and a discussion about the limitations of the model, as well as possible extensions of the approach.

2 Theory

Here we introduce the theoretical framework used throughout this work. We begin by presenting the tight-binding model for electrons in a two-dimensional square lattice and how distance-dependent hopping leads to electron-phonon coupling. We then introduce thermodynamic expressions based on the Helmholtz free energy and show how the electronic structure can be connected to lattice forces and interatomic force constants.

2.1 Tight-Binding Approximation

The tight-binding model has its origin in the quantum mechanical description of electrons in a periodic potential, where the wavefunctions are approximately localized around atomic sites, following the work of Slater and Koster [11]. Although the electrons are strongly localized around the atomic sites, they are able to tunnel, also known as hop, to other sites based on interatomic distance. Generally, the hopping amplitude decreases with increasing interatomic distance due to the reduced overlap of atomic orbitals. In this work, we use the approximation of retaining only nearest-neighbor hopping terms and neglect longer-range hopping interactions, leading to simplified calculations while remaining physically relevant. Despite its simplicity, the tight-binding approximation has been shown to reproduce properties such as energy bands and gaps [12].

Within this approximation, the Hamiltonian is written as a sum over nearest-neighbor hopping as

$$H = \sum_{\langle i,j \rangle} t_{ij} [\, \hat{c}_i^\dagger \hat{c}_j + \hat{c}_j^\dagger \hat{c}_i] \tag{1}$$

where $c_i^\dagger$, c_i are creation and annihilation operators which increase, and respectively decrease, the number of electrons at a specific atomic site by one [13].

In modern approaches, tight-binding Hamiltonians have been systematically derived from first-principles calculations through downfolding techniques based on Wannier functions. This procedure both preserves essential physics of the system while also reducing computational complexity, and has been applied to systems with strong electron-lattice coupling and charge density wave instabilities [14].

In this work we consider a two-dimensional square lattice of size $L_x \times L_y$ with lattice constant a. Electron motion is described within a nearest-neighbor tight-binding model with hopping amplitude t. Phonons are encoded in the force-constant tensor $\Phi_{ij}^{\alpha\beta}$, where i, j denote lattice sites and α, β are Cartesian components. The full model is illustrated in Figure 1

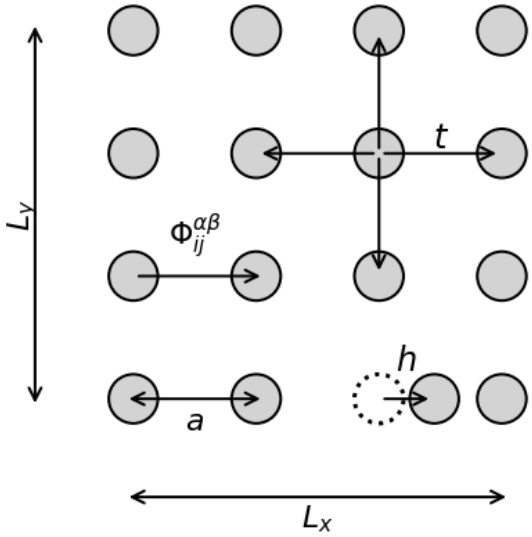

Figure 1: Schematic illustration of the square lattice model used in this work. The system consists of a lattice of size $L_x \times L_y$ with lattice constant a. Electrons can hop between nearest-neighbor sites with hopping amplitude t. The force constant tensor $\Phi_{ij}^{\alpha\beta}$ coupling sites i and j and atomic displacement variable h is also shown. The displacement is exaggerated for visualisation and does not represent actual distance used.

2.2 Distance-dependent Hopping and Electron-Phonon Coupling

The positions of atoms in real materials are not fixed, and instead constantly vibrate around their equilibrium positions. This leads to group movements in the lattice where the interatomic distances constantly change. The probability for an electron to hop between neighboring sites depends on this distance and is thus effectively a function of interatomic separation, as illustrated in Figure 1. We can model this dependence by introducing a linear parameter α that controls the strength of the electron-phonon coupling. Consequently, any atomic displacement modifies the total electronic energy of the lattice, where the energy difference then originates from the restoring forces of the collective atomic springs.

3 Methodology

This section presents computational methodology used to evaluate the force constants. A description is made of the tight-binding Hamiltonian, calculation of the free energy and numerical extraction of force constants using finite-displacement. We also discuss symmetry-based simplifications, numerical considerations and the relation of the force constant matrix and lattice dynamics.

3.1 Free Energy from a Tight-Binding Model

We consider a periodically bound two-dimensional square lattice with interatomic spacing a, where the electrons are tightly bound to the atomic sites, but are able to hop between neighboring sites with hopping amplitude t. Here, we restrict ourselves to a linear model, although more detailed approaches exist [11,12,14]. The amplitude of the hopping between neighboring sites i and j then depends on their interatomic distance [8, 9] r_{ij} as

$$t_{ij} = -t_0 \left(1 - \alpha(r_{ij} - r_0)\right) \tag{2}$$

where t_0 is the hopping amplitude when the neighboring sites are at their equilibrium positions, r_0 is the equilibrium distance, and α is a parametrization of the electron-phonon coupling strength, set to $\alpha = 0.01$ in our model. This choice of α represents a weak electron-phonon coupling regime, where changes in interatomic distance produce small variations in the hopping amplitude. We consider the Hamiltonian mentioned in Equation 1 and for a given set of atomic positions, diagonalization of the Hamiltonian yields the eigenvalues ϵ_n and eigenstates $|\psi_n\rangle$ of the system

$$H\,|\psi_n\rangle = \epsilon_n\,|\psi_n\rangle \tag{3}$$

At zero temperature, the electronic states are filled up to the Fermi level, and thus the total energy is given by the sum of the total number of electrons N_e lowest eigenvalues.

$$E = \sum_{n=1}^{N_e} \epsilon_n \tag{4}$$

At a finite temperature T the occupation of each eigenstate follows the Fermi-Dirac distribution [15], expressed by the Fermi function f_d, where k_B is the Boltzmann constant and μ is the chemical potential

$$f_d = \frac{1}{\exp\left(\frac{\epsilon_n - \mu}{k_B T}\right) + 1}, \tag{5}$$

leading to the more general expression

$$E = \sum_{n=1} f_d \epsilon_n \tag{6}$$

If we then consider the entropy S of the system

$$S = -k_B \sum_n \left[f_d \ln(f_d(n)) + (1 - f_d(n)) \ln(1 - f_d(n))\right] \tag{7}$$

the Helmholtz free energy F is given by

$$F = E - TS \tag{8}$$

which provides a connection between the electronic structure and thermodynamic properties of the system.

3.2 Extraction of Force Constants

The interatomic forces between atoms i and j, also known as the force constants $\Phi_{ij}^{\alpha\beta}$, where α, β denote Cartesian directions, are defined as the second derivatives of the free energy with respect to atomic displacements $x_{i\alpha}, x_{j\beta}$ from their equilibrium positions

$$\Phi_{ij}^{\alpha\beta} = \frac{\partial^2 F}{\partial x_{i\alpha} \partial x_{j\beta}} \tag{9}$$

To compute these mixed derivatives numerically, we use the second order central difference approximation for $F(x, y)$

$$\frac{\partial^2 F}{\partial x \partial y} \approx \frac{F_{--} + F_{++} - F_{+-} - F_{-+}}{4h^2} \tag{10}$$

where h represents small displacements of the two atoms along the negative $(-)$ or positive $(+)$ Cartesian direction

$$F_{\pm\pm} = F(x \pm h, y \pm h) \tag{11}$$

For the diagonal on-site terms, the centered difference approximation is

$$\frac{\partial^2 F}{\partial x^2} \approx \frac{F(x+h) + F(x-h) - 2F(x)}{h^2} \tag{12}$$

Consequently, by numerically displacing all individual pairs of atoms, the full force constant matrix can be assembled.

3.3 Symmetry Considerations, Choice of Units and Computational Simplifications

The square lattice used in this work has several symmetries which can be utilized. Since we have imposed periodic boundary conditions, all atomic sites are equivalent. The force constants do not depend on absolute positions, but only on their relative interatomic distances. Consequently, it is often sufficient to only calculate the forces for a single reference atom, since the force constants depend only on the relative separation between atoms (Δ_x, Δ_y) and then generalize the results to the entire lattice. In addition to translational invariance, the square lattice exhibits discrete rotational symmetry under 90° rotations (C_4 symmetry) when the hopping amplitudes are equal, $t_x = t_y$. Under such rotations, the force constant matrices transform accordingly, reflecting the symmetry of the underlying lattice. Although the individual Cartesian components of the tensor depend on the chosen coordinate system, its eigenvalues remain invariant under rotation.

These symmetry properties can significantly reduce the number of force constants that need to be computed, which in itself is a computationally heavy task, due to multiple diagonalization of the Hamiltonian. In the ideal lattice these symmetries are exact, but

some numerical deviations may arise due to finite lattice size and numerical differentiation. Nevertheless, these symmetry relations provide both faster computations and work as a guideline for validating results.

For convenience we generally set the hopping amplitude to $t_0 = 1$. This simplification leads to the hopping amplitude setting the energy scale of the system, as the eigenvalues of the tight-binding Hamiltonian scale with t. Since the thermal occupation is determined by the Fermi-Dirac distribution, with relevant dimensionless quantity $(\epsilon - \mu)/k_B T$, if we set the Boltzmann constant to $k_B = 1$, the temperature is also expressed in terms of the hopping amplitude. This allows us to explore temperature dependence without introducing excessive scaling factors into the computations.

3.4 Matrix Structure of Φ and its Relation to Phonons

The force constants $\Phi_{ij}^{\alpha\beta}$ obtained in this work can be viewed as elements of a real-space matrix that describes the linear response of the lattice to small atomic displacements. For a system with N number of atoms, this object can be arranged into a $2N \times 2N$ matrix, where each 2×2 block contains information about the interaction between atom i and atom j in directions α, β, forming a 2×2 tensor in Cartesian coordinates. This structure directly relates to lattice dynamics within the harmonic approximation, since the equations of motion for small atomic displacements can be written in terms of the force constants as coupled sets of linear equations. The forces acting on each atom are determined by the displacements of all other atoms through the force constant $\Phi_{ij}^{\alpha\beta}$. Therefore the force-constant matrix acts as an effective stiffness matrix of the lattice, determining how perturbations propagate through the system.

It is common to transform real-space force constants into momentum space via Fourier transforms, leading to the so called dynamical matrix $D(q)$. The eigenvalues of this matrix give access to phonon dispersion relations, and its eigenvectors describe the polarization and relative motion of atoms within each of the vibrational modes. However, this step is not performed in the present work since the real-space force constant matrix contains the same physical information in an equivalent representation.

In this sense, the forces computed in this thesis can be interpreted as the real-space foundation of phonon physics. The spatial decay, structure and temperature dependence of $\Phi_{ij}^{\alpha\beta}$ directly reflect how phonons would behave in momentum space. Since the present analysis remains entirely in real-space, the focus is placed on direct interpretation of interaction strengths rather than phonon band structures.

It is also worth noting that the model does not originate from an explicit interatomic potential, but instead emerges from the electronic Helmholtz free energy. The resulting lattice dynamics are therefore effectively electron-mediated, determined by the underlying electronic structure and its coupling to phonons. While the force constants are obtained from a quantum-mechanical free energy, the atomic displacements are treated classically within the Born-Oppenheimer and harmonic approximations, leading to a classical harmonic lattice model.

4 Results and Discussion

In this section, we provide discussion and analysis of the results obtained from our simulations. For simplicity, as previously mentioned, the base hopping amplitude, Boltzmann constant, and hopping parametrization are set to $t_0 = 1$, $k_B = 1$, $h = 0.01$, and $\alpha = 0.01$ respectively, unless otherwise stated. Consequently, temperature is expressed in units of the hopping amplitude and should be interpreted as a model parameter rather than a physical temperature in Kelvin. While a real materials electronic bandwidth could be implemented, the higher temperature ranges used in some of the figures would in general be unrealistic for solid materials. The temperature ranges are instead used to explore crossover behavior of our model, from low temperature where the Fermi surface is sharply defined, to a high-temperature regime where thermal broadening progressively suppresses the electronic response and resulting force constants.

Furthermore, while a larger lattice size yields more accurate results, they also significantly increase computational cost. Therefore, a compromise between computational efficiency and accuracy was implemented, which resulted in a size of $L_x = L_y = 19$ with a minimum temperature of $T = 0.2$ being used. Here the minimum temperature is based on the range of eigenvalues with respect to the number of atoms for the 19×19 lattice. This was done to minimize finite-size effects due to temperatures near zero, and a larger lattice size would be able to handle lower temperatures.

4.1 Harmonic Regime

To verify the validity of the harmonic approximation and the numerical method used to extract the force constants, we first examine the dependence of the Helmholtz free energy on small atomic displacements. The free energy can be expanded as a Taylor series in the atomic displacements near equilibrium. Since the first derivatives vanish at equilibrium, the contribution will be mostly from second order contributions, implying a quadratic dependence of the free energy within the harmonic regime.

Figure 2(a) shows the change in Helmholtz free energy, ΔF as a function of displacement h. The free energy exhibits an approximately quadratic dependence in this range, centered around the equilibrium position. This behavior is consistent with the harmonic approximation, indicating that restoring forces remain linear for sufficiently small distortions.

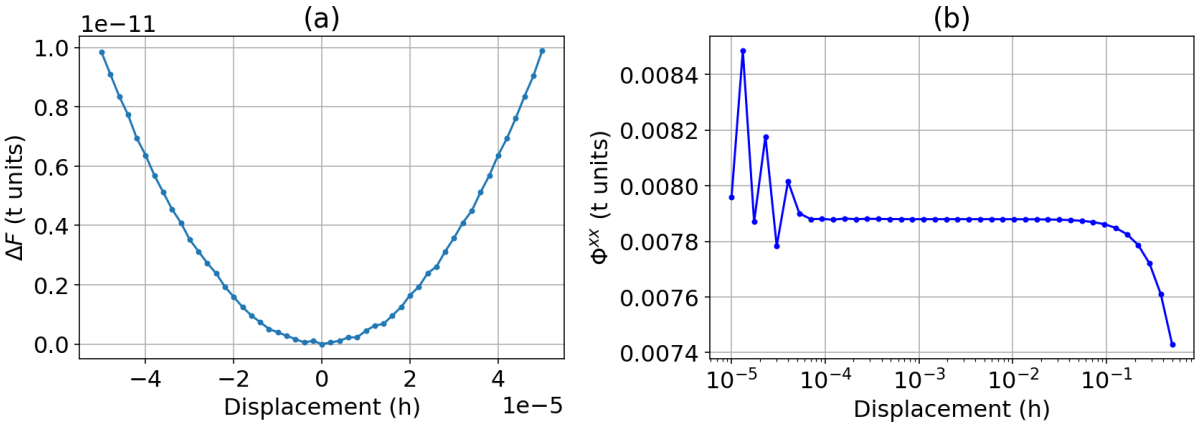

Figure 2: Change in Helmholtz free energy ΔF as a function of atomic displacement h (a), together with the corresponding on-site force constant Φ^{xx} (b). The rest of the parameters used in producing the plots were $L_x, L_y = 19$, $T = 0.2$, $\mu = 0$ and $t_0 = 1$.

To test the numerical stability of the finite-difference method, we also evaluate the on-site force constant Φ^{xx} as a function of displacement h over the same range, as shown in Figure 2(b). Over the interval $h \in [10^{-4}, 10^{-2}]$, the extracted force constant is approximately invariant. Within this regime, Φ^{xx} remains stable showing negligible numerical fluctuations, indicating convergence of the finite-difference approximation.

For displacement magnitudes smaller than this interval, the extracted force constants become increasingly sensitive due to numerical precision errors. On the other hand, for larger displacement magnitudes, the finite-difference approximation gradually loses accuracy as the displacements probe a wider region. Although the free energy itself retains an approximately quadratic form over the full range, the numerical estimation of the second derivatives becomes less reliable outside of $h \in [10^{-4}, 10^{-2}]$. This identified interval therefore defines a numerically stable range in which the finite-difference approximation provides consistent force constants. Consequently, displacement magnitudes within this range are used throughout the remainder of this work. Whereas this full interval produces stable results, the upper bound is preferred because it minimizes numerical artifacts caused by division near zero.

4.2 Spatial Structure of the Force Constants

To investigate the spatial structure of the interatomic interactions, we compute the force constant $\Phi_{ij}^{\alpha\beta}$ between a reference atom and all other atomic sites, where every interaction is described by a 2×2 tensor in Cartesian space. For each 2×2 force-constant block, we define the dominant eigenvalue as the eigenvalue with the largest magnitude, while retaining its original sign, and use this quantity as a scalar measure of the interaction strength. Consequently the dominant eigenvalue characterizes both strength and direction of the largest restoring response between each atomic pair. Figure 3 shows the resulting spatial distribution for varying temperatures.

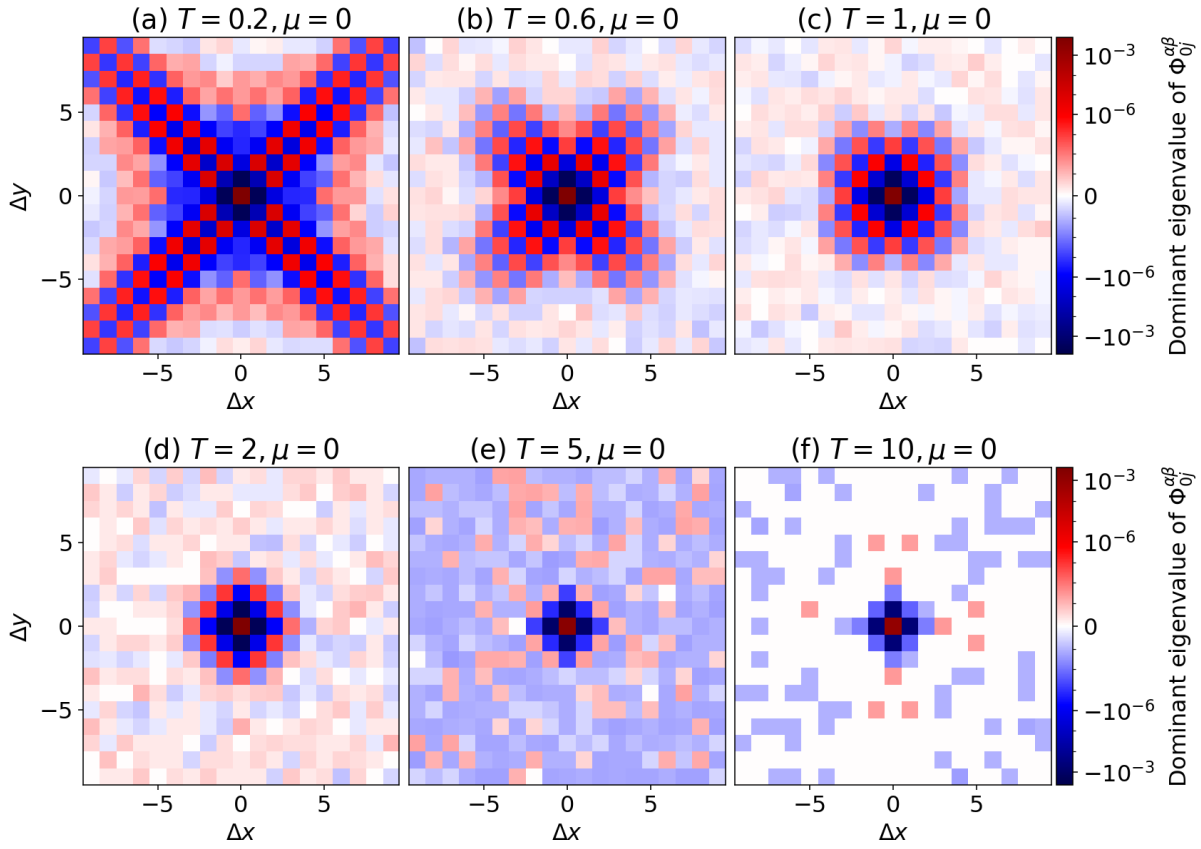

Figure 3: Spatial distribution of the dominant eigenvalue of the interatomic force-constant tensor, relative to a fixed centered reference atom indexed as 0 at position $(0, 0)$. Each lattice point represents the largest absolute eigenvalue of the corresponding 2×2 force-constant block, providing a measure of the strongest response between atomic pairs. Results are shown for $T = 0.2$ (a), $T = 0.6$ (b), $T = 1$ (c), $T = 2$ (d), $T = 5$ (e), and $T = 10$ (f), where all temperatures are given in units of the hopping amplitude. Note that very small eigenvalues are included in the plots, leading to some visually apparent asymmetries, especially at high temperature. The remaining parameters used to produce the plots were $L_x = L_y = 19$, $h = 0.01$, $\mu = 0$ and $t_0 = 1$.

The temperature range here is not intended to correspond to realistic physical temperatures, but rather as a means to explore the mathematical behavior of our model. At low temperature ($T = 0.2$), the force constants display a long-range structure with an X-shaped pattern extending across the lattice. The electron-mediated forces are direction-dependent and enhanced along specific directions. The nature of the force constants is a consequence of the underlying electronic structure of the square lattice. At low temperature, the Fermi-Dirac distribution is sharp and only electronic states in close proximity to the Fermi level contribute to the free energy. Consequently, the force constants become sensitive to the geometry of the Fermi surface and the symmetry of the electronic dispersion. For a square lattice TB-model, the electronic structure is inherently diamond-shaped in momentum space. This four-fold symmetry is then reflected in real space through directional, long-range interactions at low temperature.

As the temperature increases the range of the forces rapidly decreases due to thermal

broadening of the electronic occupation. The electronic response to atomic displacements becomes less sensitive, which results in the interactions being more short-ranged. At high temperatures the thermal broadening of the Fermi-Dirac distribution reduces the sensitivity of the free energy to atomic displacements significantly. The magnitude of the force constants decreases rapidly with distance for increasing temperature, where the resulting forces become increasingly localized to nearest neighbors only. It is worth noting that many of the eigenvalues are very small due to very weak interactions, which become even more prominent at increasing temperatures, leading to many of the figures having visually apparent asymmetries.

Overall, the interatomic force constants are strongly governed by temperature, affecting both range and magnitude.

4.3 Chemical Potential Dependence of the Force Constants

To analyze how the electron filling influences the spatial structure of the interatomic interactions, we compute the force constant tensor for different values of the chemical potential μ. The chemical potential determines the Fermi level within the band structure, directly influencing the geometry of the occupied states contributing to the free energy response.

Figure 4 shows the spatial distribution of the force constants for $\mu = -3$ at varying temperatures. The results are identical for positive and negative values of the chemical potential of same magnitude, indicating particle-hole symmetry of our TB-model when $t_x = t_y$. Thus the force constants depend primarily on the relative filling of electronic states around the Fermi level, rather than the sign of μ.

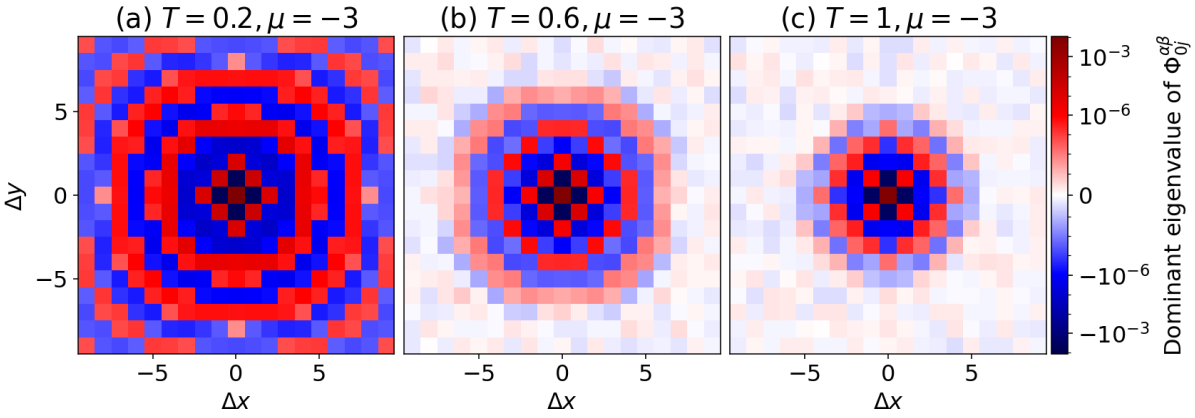

Figure 4: Spatial distribution of the dominant eigenvalue of the interatomic force-constant tensor, relative to a fixed centered reference atom indexed as 0 at position $(0, 0)$ for chemical potential $\mu = -3$. Each lattice point represents the largest absolute eigenvalue of the resulting 2×2 force-constant block, providing a measure of the strongest response between atomic pairs. Results are shown for $T = 0.2$ (a), $T = 0.6$ (b), and $T = 1$ (c), where all temperatures are given in units of the hopping amplitude. The remaining parameters used to produce the plots were $L_x = L_y = 19$, $h = 0.01$ and $t_0 = 1$.

In this regime of chemical potential, the force constants exhibit a pronounced oscillatory structure, which is characterized by alternating ring-like patterns of positive and negative

values around the reference atom. These spatial oscillations indicate that the forces now have a strong radial dependence as opposed to the more directional pattern at half-filling. The structure is reminiscent of Friedel-like oscillations [2], i.e. an oscillatory real-space response arising from the sharp Fermi surface of metallic systems. Oscillations like these are typically associated with non-local screening effects mediated by electronic states near the Fermi level. As the temperature increases, the range of the force constants become increasingly restricted, as previously discussed in section 4.2.

Figure 5 shows the spatial distribution of the force constants at low temperature for increasing μ.

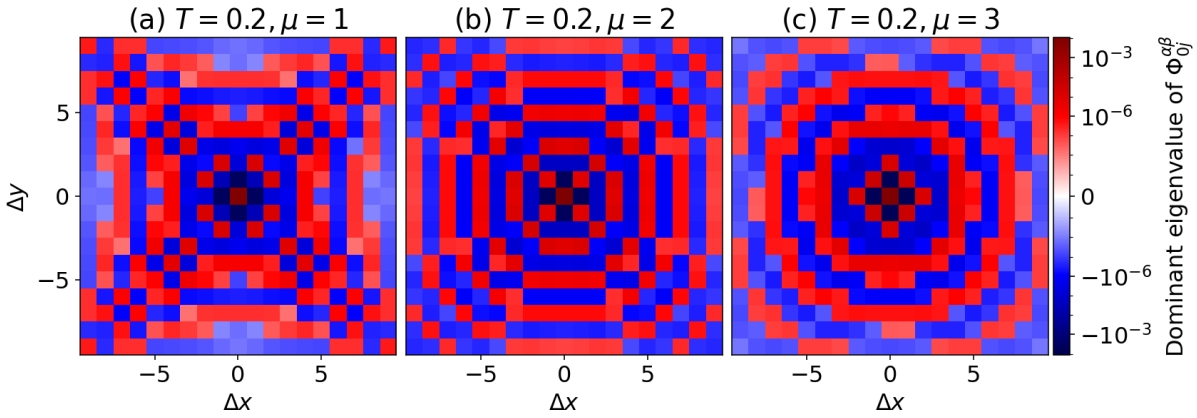

Figure 5: Spatial distribution of the dominant eigenvalue of the interatomic force-constant tensor, relative to a fixed centered reference atom indexed as 0 at position $(0, 0)$ for chemical potential $\mu = 1$ (a), $\mu = 2$ (b), and $\mu = 3$ (c). Each lattice point represents the largest absolute eigenvalue of the resulting 2×2 force-constant block, providing a measure of the strongest response between atomic pairs. The remaining parameters used to produce the plots were $L_x = L_y = 19$, $T = 0.2$, $h = 0.01$ and $t_0 = 1$.

For $\mu = 1$ the force constants show signs of the same X-shaped features as $\mu = 0$ in Figure 3, while increasing chemical potential gradually move further towards the ring-shaped pattern from Figure 4. Thus the chemical potential governs symmetry and oscillatory response. As the chemical potential increases, the electronic states shift deeper into the band structure, where the dispersion is increasingly rounded in momentum space.

4.4 Finite-Size Effects

Since the tight-binding model is evaluated on a finite $L_x \times L_y$ lattice with periodic boundary conditions, our results are subject to the influence of discretization effects. In the thermodynamic limit, the electronic states form continuous bands, but for a finite lattice the allowed states are directly related to the size of the system. Consequently, the thermodynamic properties obtained from the electronic structure also has a size dependence. An illustration of this effect can be seen in Figure 6, where the density of states obtained from the Hamiltonian eigenvalues are shown for $L_x = L_y = 10$ (a) and $L_x = L_y = 80$ (b).

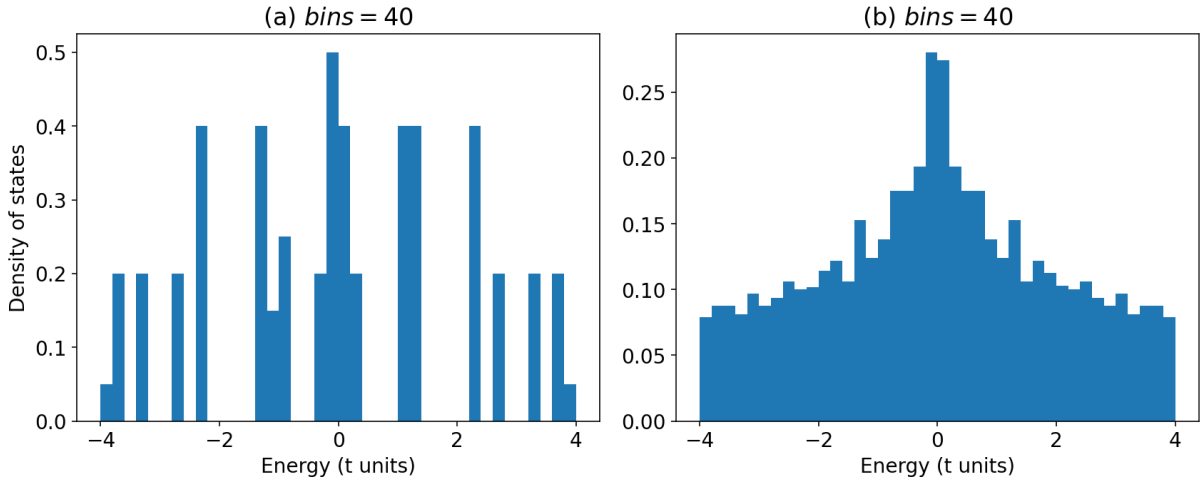

Figure 6: The electronic density of states constructed from the Hamiltonian eigenvalues for $L_x = L_y = 10$ (a) and $L_x = L_y = 80$ (b) using 40 equally spaced bins. The remaining parameters used to produce the plots were $h = 0.01$ and $t_0 = 1$

For smaller lattice sizes, the spectrum consist of a discrete set of eigenvalues. As the system grows in size, the density of states become smoother, approaching the continuous distribution expected in the thermodynamic limit. As the free energy depends on the full eigenvalue spectrum, this directly affects our thermodynamic quantities.

For the spatial structure, a smaller lattice size provide less information of the emerging patterns, but did not show any other discrete effects. This is visualized by using varying lattice sizes with otherwise fixed parameters in Figure 7.

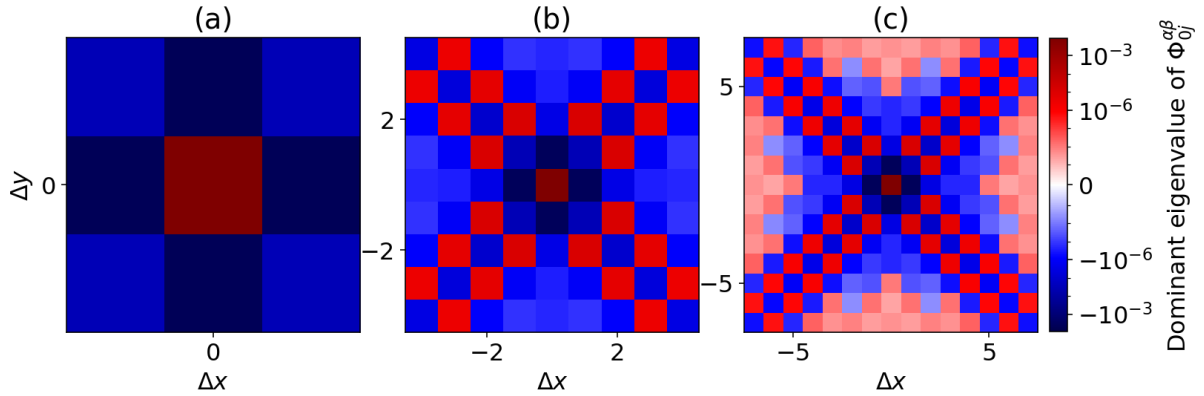

Figure 7: Spatial distribution of the dominant eigenvalue of the interatomic force-constant tensor, relative to a fixed centered reference atom at position (0,0) using varying lattice sizes. Each lattice point represents the largest value of the resulting 2×2 force-constant block, providing a measure of the strongest response between atomic pairs. Results are shown for $L_x = L_y = 3$ (a), $L_x = L_y = 9$ (b) and $L_x = L_y = 15$ (c). The remaining parameters used to produce the plots were $T = 0.2$, $h = 0.01$, $\mu = 0$ and $t_0 = 1$.

These discretization effects propagate into the force constants, as they are derived from the free energy. To quantify the extent to which this will affect our results, we examine the on-site, $|\Delta x| = 1$ and $|\Delta x| = 2$ force constant Φ^{xx} as a function of lattice size in Figure 8.

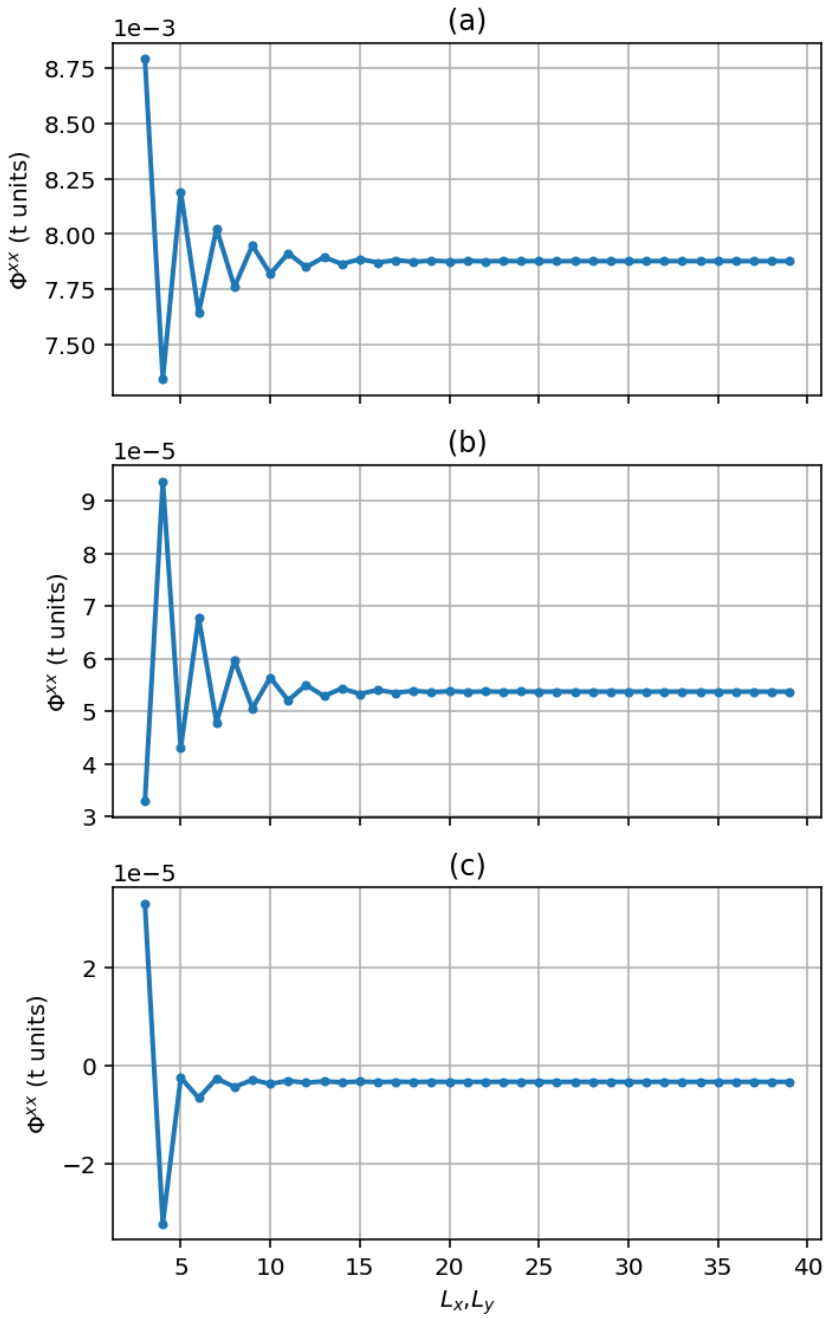

Figure 8: Force constant Φ^{xx} as a function of lattice size of the on-site (a), $|\Delta x| = 1$ (b), and $|\Delta x| = 2$ (c) interactions, in Cartesian x-direction. The remaining parameters used to produce the plots were $T = 0.2$, $h = 0.01$, $\mu = 0$ and $t_0 = 1$.

The results show that the magnitude of the force constants converges rapidly with increasing lattice size and remain consistent among these interatomic interactions. The larger jumps between consecutive smaller lattice sizes originate from the lattice periodicity and the fact that the size switches from even to odd.

Although Figure 8 only shows a selection of force constants, similar convergence was observed across representative elements of the force-constant matrix. As the force constants become quite stable for lattice sizes around $L_x = L_y > 15$, this suggests that the general trends of the force constants are already well captured even at moderate L_x and L_y, where

these trends are the main interest of this thesis. An increased lattice size also reduces the influence of interactions with periodic images due to the periodic boundary conditions.

Since the force constants are obtained from repeated diagonalization of the tight-binding Hamiltonian, the computational cost increases substantially with lattice size. Based on this analysis, the lattice size $L_x = L_y = 19$ was chosen to represent most of this work. This size covers the general spatial trends of the force constants while also maintaining both numerical consistency and efficiency. It should be emphasized that this convergence analysis establishes numerical stability for this simple model and does not imply that the size is sufficient for more realistic models.

4.5 Temperature Dependence and Scaling of the Force Constants

As seen in the previous sections, the force constants diminish as the temperature of the system increases. Here we take a closer look at this behavior by examining some of the major forces affecting a reference atom. Figure 9 shows the force constants Φ^{xx} and Φ^{yy} for on-site, $|\Delta x| = 1$ and $|\Delta x| = 2$ at increasing temperature. Due to the previously discussed symmetry of the lattice, this holds for any reference atom with neighbors defined along the Cartesian x-direction.

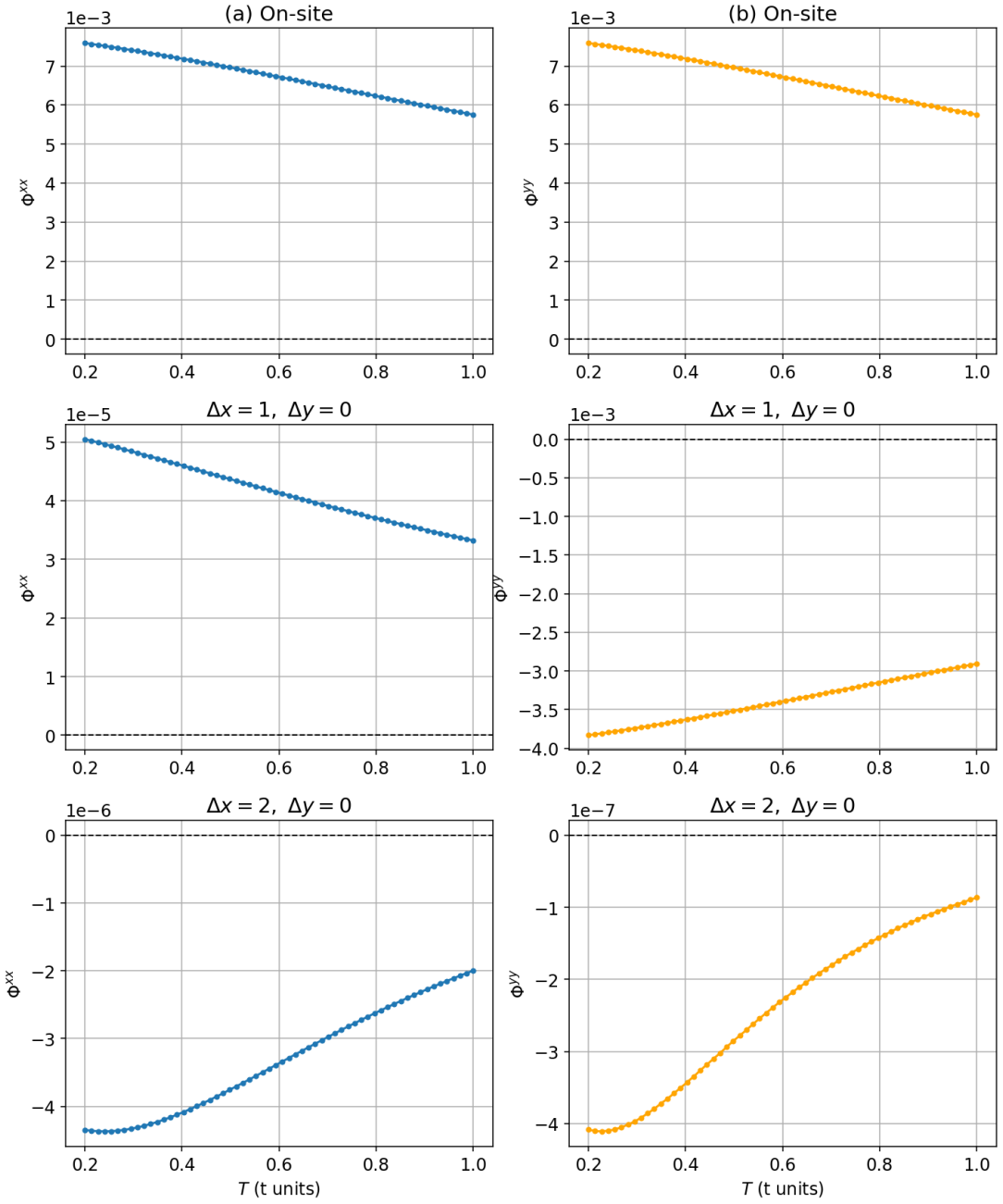

Figure 9: Temperature dependence of the force constants Φ^{xx} and Φ^{yy} for the on-site (a),(b), $|\Delta x| = 1$ (c),(d) and $|\Delta x| = 2$ (e),(f), interactions, in Cartesian x-direction. The remaining parameters used to produce the plots were $L_x = L_y = 19$, $h = 0.01$, $\mu = 0$ and $t_0 = 1$.

As expected, the force constants show a direct relation to temperature, exhibiting a power-law like distribution where rising temperature leads to diminished magnitude. In Figure 10 we plot the magnitude of the same force constants on logarithmic scales, combined with a curve fit to $c/T + d/T^2$, where c and d are fitting parameters. The fitting function was chosen as a simple low-order approximation based on theoretical expectation and numerical observation. At high temperature the thermodynamic quantities can be expanded in inverse powers of temperature, leading to a contribution proportional to $1/T$ together with higher-order corrections. The approximately linear behavior observed on logarithmic scales also indicate power-law decay of the force constants with temperature.

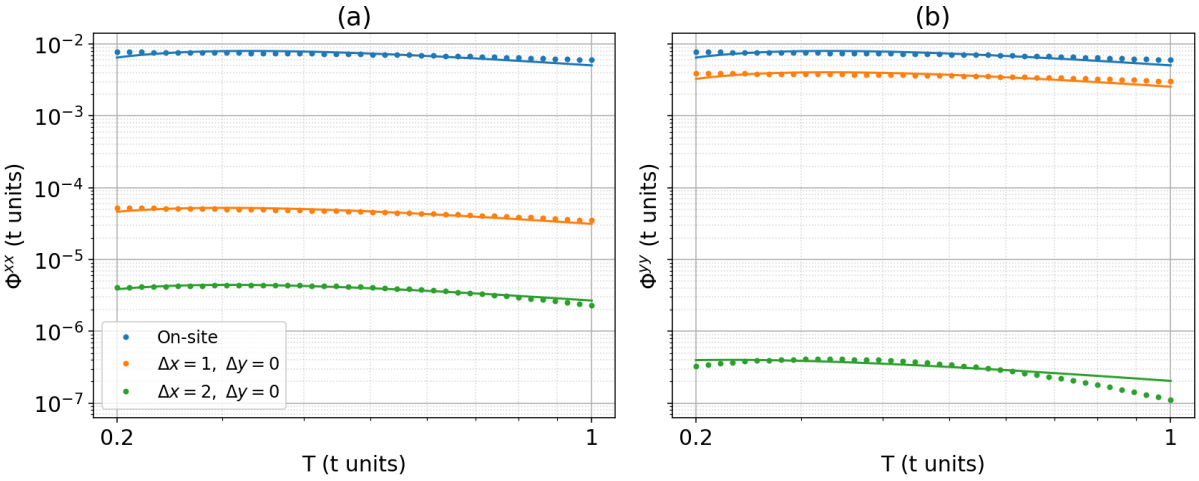

Figure 10: Temperature dependence of the force constants Φ^{xx} and Φ^{yy} for the on-site, $|\Delta x| = 1$ and $|\Delta x| = 2$ interactions in Cartesian x-direction on logarithmic scales. At sufficiently high temperatures, the data follow an approximately linear trend, indicating power-law behavior. Markers represent the computed data points of these major forces acting on an atom, while solid lines indicate curves fitted to $c/T + d/T^2$. The remaining parameters used to produce the plots were $L_x, L_y = 19$, $h = 0.01$, $\mu = 0$ and $t_0 = 1$.

The fitted curve captures the dominant trend, but deviations indicate that the scaling is not fully captured by this low-order approximation alone. It is worth noting that in Figure 10 values below a threshold of 10^{-8} have been omitted due to discretization effects.

4.6 Effects of Anisotropic Hopping

In this section we investigate how anisotropy in the hopping amplitudes influences the force constants. In Figure 11 we introduce direction-dependent hopping amplitudes t_x and t_y along their respective Cartesian direction.

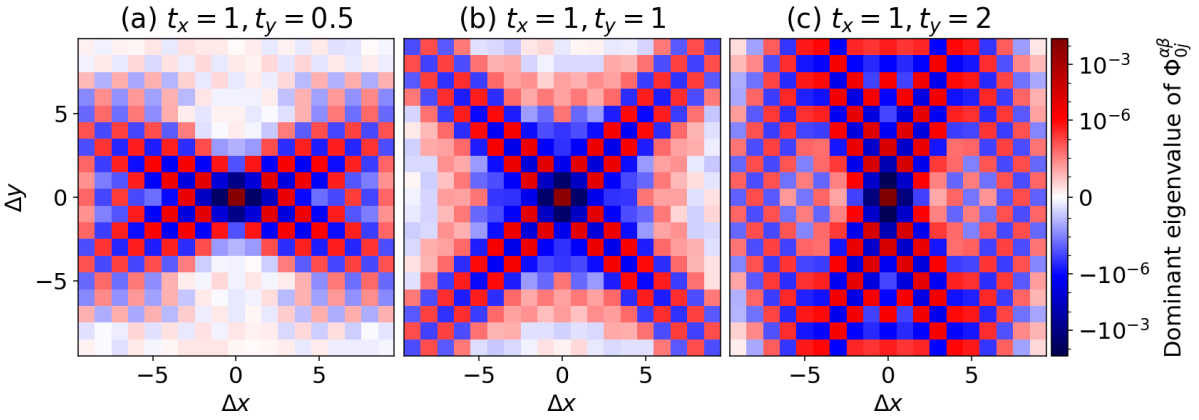

Figure 11: Spatial distribution of the dominant eigenvalue of the interatomic force-constant tensor, relative to a fixed centered reference atom indexed as 0 at position $(0, 0)$ using varying directional hopping amplitudes t_x and t_y at $\mu = 0$. Each lattice point represents the largest absolute eigenvalue of the resulting 2×2 force-constant block, providing a measure of the strongest response between atomic pairs. The remaining parameters used to produce the plots were $L_x = L_y = 19$, $T = 0.2$ and $h = 0.01$.

As the hopping amplitude decreases along a specific direction, the electronic coupling between sites along the same direction weaken, which is then reflected in the force constant propagation. Conversely, as the hopping amplitude increases the coupling is enhanced. The results demonstrate that anisotropy in the hopping amplitudes is directly reflected in the structure of the force constants. Given that the tight-binding dispersion relation is

$$\epsilon(k_x, k_y) = -2t_x \cos(k_x a) - 2t_y \cos(k_y a) \tag{13}$$

this makes sense, as the curvature of the electronic states become direction-dependent if $t_x \neq t_y$. For a square lattice model, at half filling the sign of the hopping can be absorbed through symmetry transformations, leading to the force constants being primarily governed by the relative magnitude of t_x and t_y, and not their sign. Away from half-filling, this symmetry breaks and the force constants acquire a dependence on both hopping structure and chemical potential, albeit rather small for our model, which can be seen for $\mu = 1$ in Figure 11.

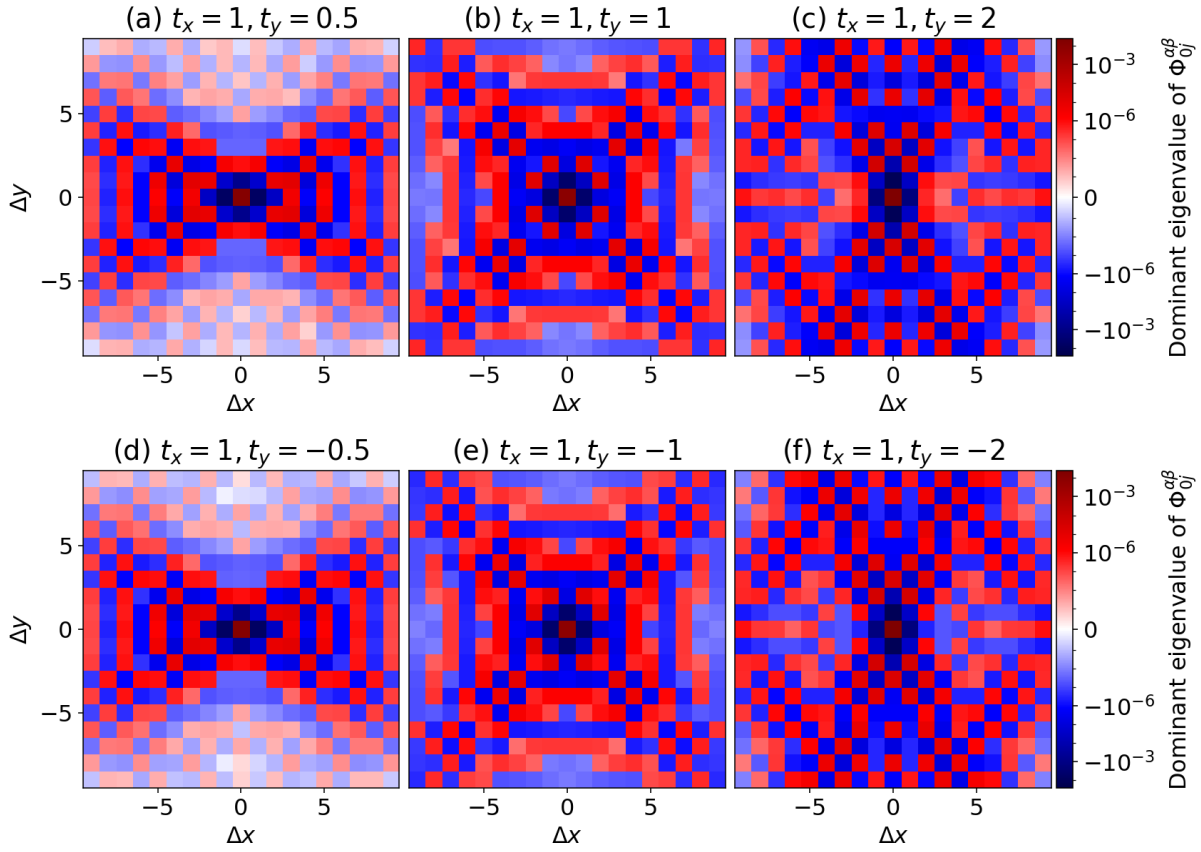

Figure 12: Spatial distribution of the dominant eigenvalue of the interatomic force-constant tensor, relative to a fixed centered reference atom indexed as 0 at position $(0, 0)$ using varying directional hopping amplitudes t_x and t_y at $\mu = 1$. Each lattice point represents the largest absolute eigenvalue of the resulting 2×2 force-constant block, providing a measure of the strongest response between atomic pairs. The remaining parameters used to produce the plots were $L_x = L_y = 19$, $T = 0.2$ and $h = 0.01$.

5 Conclusion and Outlook

In this thesis, we studied the electron-mediated interatomic force constants within a square two-dimensional tight-binding model with distance-dependent hopping. By modeling the electronic contribution through the Helmholtz free energy and evaluating its second derivatives with respect to atomic displacements, we constructed a real-space force constant matrix containing information about the force structure of the system. We have provided analysis and interpretation over which variables govern these force constants.

All calculations were implemented in custom numerical code, where the tight-binding Hamiltonian was constructed and diagonalized for each atomic configuration. From the resulting eigenvalue spectrum, the free energy was computed, and interatomic force constants were extracted using finite-difference differentiation. The simulations were performed on finite lattices with typical runtimes of up to approximately 4 minutes on a standard personal laptop, depending on system size and quantity being plotted.

The results show that the force constants are sensitive to thermodynamic conditions and the underlying electronic structure. Low temperature exhibits long-range force constants that reflect the sharpness of the Fermi surface. Increasing temperature reduces the sensitivity by thermal smearing, leading to suppression of long-range behavior with a transition to the forces becoming more localized. Changes in band filling affect the spatial structure of the force constants. At near half-filling, the force constants have a directional structure, reflecting the rotational symmetry of the lattice. With increasing magnitude of the chemical potential, the spatial dependence becomes more oscillatory and radially symmetric instead, reminiscent of Friedel-like screening in metallic systems. We also demonstrated that anisotropy in the hopping amplitudes is directly reflected in the real space forces.

Several extensions of this work are possible. Different lattice geometries could be implemented, such as triangular or honeycomb lattices, which would lead to different force-constant structures. The model could be extended to three dimensions, which would enable closer comparison to similar real crystalline materials. A further extension would be to include a multi-atom basis, allowing the study of optical phonon modes in addition to the acoustic ones. This would also allow the model to connect to more direct experimental quantities such as Raman spectra. Establishing a connection between the real-space force constants and their momentum-space representation would allow additional insight into phonon dispersion relations and better comparison to scattering experiments.

Beyond this, there are also larger improvements that could be implemented, such as using more advanced electronic structure models. Nevertheless, the present work demonstrates that even a minimal model can capture electron-mediated force structures and provide insight into electron-phonon coupled systems.

References

[1] R. Heid. Electron-phonon coupling. 2017. Accessed 2026-03-20, available at: `http://www.cond-mat.de/events/correl17/manuscripts/heid.pdf`.

[2] J. Friedel. The distribution of electrons round impurities in monovalent metals. *The London, Edinburgh, and Dublin Philosophical Magazine and Journal of Science*, 43(337):153–189, 1952.

[3] M. A. Ruderman and C. Kittel. Indirect exchange coupling of nuclear magnetic moments by conduction electrons. *Phys. Rev.*, 96(1):99–102, 1954.

[4] T. Kasuya. A theory of metallic ferro- and antiferromagnetism on zener's model. *Progress of Theoretical Physics*, 16(1):45–57, 1956.

[5] K. Yosida. Magnetic properties of cu-mn alloys. *Phys. Rev.*, 106(5):893–898, 1957.

[6] W. Kohn. Theory of the insulating state. *Phys. Rev.*, 133:A171–A181, 1964.

[7] M. Born and R. Oppenheimer. Zur quantentheorie der molekeln. *Annalen der Physik*, 389(20):457–484, 1927.

[8] S. Froyen and W. A. Harrison. Elementary prediction of linear combination of atomic orbitals matrix elements. *Phys. Rev. B*, 20:2420–2422, 1979.

[9] W. A. Harrison and S. Froyen. Universal linear-combination-of-atomic-orbitals parameters for *d*-state solids. *Phys. Rev. B*, 21:3214–3221, 1980.

[10] R. Xu and T. C. Chiang. Phonon studies by x-ray thermal diffuse scattering. *Zeitschrift für Kristallographie*, 220:1009–1016, 2005.

[11] J. C. Slater and G. F. Koster. Simplified lcao method for the periodic potential problem. *Phys. Rev.*, 94(6):1498–1524, 1954.

[12] M. Elstner, D. Porezag, G. Jungnickel, J. Elsner, M. Haugk, T. Frauenheim, S. Suhai, and G. Seifert. Self-consistent-charge density-functional tight-binding method for simulations of complex materials properties. *Phys. Rev. B*, 58(11):7260–7268, 1998.

[13] F. Utermohlen. Tight-binding model in the second quantization formalism. 2018.

[14] A. Schobert, J. Berges, E. G. C. P. van Loon, M. A. Sentef, S. Brener, M. Rossi, and T. O. Wehling. Ab initio electron-lattice downfolding: Potential energy landscapes, anharmonicity, and molecular dynamics in charge density wave materials. *SciPost Physics*, 16:046, 2024.

[15] P. Hofmann. Solid state physics: An introduction. pages 94–99, 2015.